

LE POINT SUR...

CONCISE REVIEW PAPER

Modelling transport in reacting geochemical systems

Craig Bethke

Department of Geology, 1301 West
Green Street, University of Illinois,
Urbana, Illinois 61801, USA.

Abstract Reactive transport modelling is a powerful tool for analysing a broad variety of problems involving the migration of fluids through the Earth's subsurface. In this paper we consider the behaviour of this class of numerical models and show how they might be applied in one dimension to improve our understanding of the interaction between transport and reaction processes. The examples we present demonstrate both the potential of the models and the challenges that arise in applying them.

Keywords: Geochemical modelling, Reactive transport, Water-rock interaction, Weathering, Ground-water contamination, Petroleum reservoirs.

Résumé Modélisation du transport dans les systèmes géochimiques réactifs

La modélisation du transport réactif est un outil de première importance dans l'analyse d'une grande variété de problèmes comportant la migration des fluides à travers la sub-surface de la Terre. Dans cet article de synthèse, est étudié le comportement de cette classe de modèles numériques et nous montrons comment ces derniers peuvent être appliqués en une dimension, de manière à mieux comprendre l'interaction entre les processus de transport et de réaction. Les exemples présentés démontrent à la fois les potentialités des modèles et les défis que soulève leur application.

Mots clés : Modélisation géochimique, Transport réactif, Interaction eau-roche, Altération météorique, Contamination des eaux souterraines, Réservoirs pétrolières.

Version
française
abrégée

INTRODUCTION

NOMBRE des problèmes les plus intéressants et les plus complexes en géosciences concernent la réaction des fluides, lorsqu'ils parcourent la tranche de la subsurface. Il y a eu récemment de rapides avancées dans le développement des modèles numériques de transport réactif et dans leur application en géochimie. Dans cet article de synthèse, sont examinées les simulations qui démontrent les interactions fortes existant en une dimension entre les processus de trans-

port et les réactions qu'ils induisent, et sont explorés les incertitudes et les défis inhérents à la modélisation des phénomènes de transport réactif.

MODÈLE MATHÉMATIQUE

Dans le modèle de transport réactif en une dimension, un domaine, de coordonnées linéaires ou radiales, est discrétisé en blocs nodaux (fig. 1). Un fluide non réactif entre à une extrémité du domaine étudié, en déplaçant un fluide réactif. La simulation comporte une série de pas de temps à partir d'une

Note

Rédigée à
l'invitation du
Comité de lecture.

remise le 15 janvier 1997,
acceptée après révision
le 1^{er} avril 1997.

condition initiale, en traçant l'évolution chimique du système quand le fluide migre au travers du domaine.

Le programme évalue quatre classes d'équations par pas de temps : (1) des équations de transport qui rendent compte de la diffusion, de la dispersion hydrodynamique et de l'advection, (2) des équations d'équilibre qui décrivent la distribution de masse entre les espèces aqueuses et les minéraux, (3) un modèle d'adsorption qui prédit quels ions s'adsorbent sur les surfaces des minéraux et en quelles quantités, (4) les lois cinétiques qui prédisent la vitesse à laquelle les minéraux précipitent ou se dissolvent au cours de la simulation.

RÉACTION DANS UN AQUIFÈRE À QUARTZ

Dans un premier calcul (simulation A, **tableau II**), sont considérés les effets de l'infiltration d'eau de pluie à différentes vitesses dans un aquifère à quartz. Le fluide qui s'infiltré réagit en dissolvant le quartz en fonction d'une loi cinétique. Lorsque la réaction progresse, la concentration en silice, à chaque point de l'aquifère s'approche d'une valeur « plateau », comme le montre la **figure 2**, qui représente un équilibre entre la vitesse à laquelle la silice est transportée et celle à laquelle elle réagit. La période de relaxation nécessaire pour atteindre cet état est d'environ 0,1 an, alors que le temps nécessaire au changement notable du volume de quartz est supérieur à 10^5 ans. Ainsi, les concentrations « plateau » restent-elles presque constantes pendant de longues périodes ; les conditions de ce type, proches d'un état stable, sont connues sous le nom d'« états stationnaires ».

Pour les vitesses d'écoulement faibles (**fig. 3**), la réaction se concentre vers l'entrée et le fluide tend vers un équilibre local avec l'aquifère, après avoir migré sur une courte distance. Dans le cas d'un écoulement rapide, au contraire, le fluide traverse l'aquifère trop rapidement pour pouvoir accumuler des quantités notables de silice et approcher l'équilibre avec le quartz, et la vitesse de réaction au travers de l'aquifère reste forte. C'est pourquoi le bilan entre les vitesses de réaction et de transport exerce-t-il un contrôle de première importance sur la nature de la réaction

de l'écoulement ; ce bilan est décrit par le nombre de Damköhler.

ALTÉRATION DANS UN PROFIL DE SOL

Dans une seconde expérience numérique (simulation B, **tableau II**), a été réalisée la simulation du transport réactif pour prédire la répartition des réactions d'altération au sein d'un profil de sol. L'eau de pluie, en équilibre avec le CO_2 atmosphérique, recharge l'horizon le plus superficiel du sol, et à partir de la base, draine le fluide du système poral. Au sein du profil, le fluide maintient un équilibre avec le dioxyde de carbone du gaz du sol. Les minéraux kaolinite, gibbsite et tridymite se forment par nucléation hétérogène, en fonction des paramètres, dont la liste est fournie dans le **tableau III**.

Près de la surface, les minéraux feldspathiques se dissolvent en donnant naissance à la gibbsite et le quartz se dissout de façon congruente. A environ 25 cm, la kaolinite remplace la gibbsite en tant que piège pour l'aluminium et le quartz atteint son domaine de saturation et commence à précipiter plutôt qu'à se dissoudre. A environ 50 cm dans le profil, le polymorphe de silice qu'est la tridymite (c'est-à-dire une silice microcristalline) commence à se former, même si elle est moins stable thermodynamiquement que le quartz.

TRANSPORT D'ESPÈCES QUI S'ADSORBENT

En modélisant le transport d'espèces qui s'adsorbent, on fait ici appel à la théorie du double feuillet, plutôt qu'à l'approche plus communément utilisée, par le coefficient de répartition (K_D), qui est quelque peu plus simpliste du point de vue chimique. Dans la simulation C1 (**tableau II**), on provoque l'envahissement d'un aquifère contenant de l'oxyde ferrique par une eau contaminée en Pb et Br. Pb s'adsorbe fortement sur la surface ferrique, tandis que Br se maintient dans le fluide. Les résultats de la simulation (**fig. 5**) montrent la saturation en Pb de l'aquifère en environ 25 ans. Les résultats diffèrent de ceux que livre l'approche par K_D , principalement en ce qui concerne l'abaissement du front du Pb. Dans le processus inverse (simulation C2, **tableau II**), après la saturation en Pb de l'aquifère, ce dernier est parcouru par un fluide

propre. Si l'on applique l'approche K_D , l'effet de chasse d'eau provoque l'inverse de ce que l'on obtient par le calcul précédent (fig. 5) : le Pb se désorbe dans l'eau propre et est évacué hors du système, laissant l'aquifère à peu près pur après environ 25 ans. La simulation faisant appel au modèle du double feuillet (fig. 6) ne montre pas un tel comportement. Ainsi, le Pb se désorbe lentement, produisant un net « effet de traîne » de contamination résiduelle du fluide effluent. Après 100 ans, l'aquifère est un peu restauré et la teneur en Pb du fluide reste supérieure aux standards tolérés par la santé publique. Ces calculs suggèrent que les « effets de traîne » qui sont communément observés dans les études de transport contaminant, au laboratoire et sur le terrain, pourraient être expliqués par un processus chimique, à équilibre local.

Dans une simulation finale (C3, tableau II), on considère le phénomène de chromatographie en eau souterraine. Trois contaminants représentés par des métaux lourds, Pb, Cu, Ni, sont introduits dans un aquifère adsorbant. Les métaux entrent en compétition pour occuper les sites adsorbants et se séparent chromatographiquement (fig. 8) : Pb s'adsorbe sur les premiers sites rencontrés ; quand il y a appauvrissement en Cu. Comme les ions se déplacent aux frontières de migration entre les zones chromatographiques, Cu et Ni atteignent des concentrations supérieures à celles qui sont déterminées dans le fluide à l'entrée, ce qui conduit à des courbes de rupture complexes.

SIMULATION D'UNE INJECTION DE VAPEUR

Dans un calcul final (simulation D, tableau II), on a modélisé les effets d'une injection de vapeur sur un réservoir pétrolier clastique. L'eau chaude est forcée au travers de la formation, vers l'extérieur, en réagissant sur les minéraux du réservoir. Les minéraux réagissent en donnant naissance à un argile gonflante, la smectite, ce qui a pour effet de réduire la perméabilité (fig. 9). La décharge au travers de la formation varie, lorsque la viscosité et la perméabilité changent (fig. 10). Initialement, la décharge augmente, en réponse à la diminution de la viscosité aux abords du trou de forage, mais cet effet est contrebalancé par la perte de perméabilité

due à la formation de la smectite. Il arrive que le fluide migre plus lentement qu'avant le commencement de l'injection de vapeur.

DISCUSSION

Dans cet article de synthèse, les simulations présentées démontrent comment la modélisation peut être appliquée, précisent la nature des résultats que l'on peut attendre de la modélisation, mais elles servent aussi à mettre en évidence les défauts dans la formulation d'un modèle et les insuffisances de la théorie qui la sous-tend et des données disponibles. En simulant l'infiltration dans un aquifère à quartz, par exemple, le fluide approche l'équilibre chimique avec l'aquifère en un court intervalle de temps, même si, dans la nature, une nappe de faible profondeur est rarement en équilibre avec ce minéral. La teneur en silice d'une nappe peut être contrôlée par des réactions avec d'autres minéraux comportant de la silice, ce qui nécessite de disposer de lois cinétiques pour une variété de minéraux autres que la phase prédominante dans l'aquifère. Ainsi, dans les aquifères naturels, l'écoulement est irrégulier, parcourant rapidement certaines zones d'une formation, et lentement d'autres. En conséquence, on ne peut espérer trouver un seul nombre de Damköhler pour caractériser l'écoulement au travers des formations naturelles.

Dans le modèle d'altération météorique, en dépit du fait qu'un sol soit le siège d'une intense activité biologique, presque toutes les données cinétiques disponibles sont fournies pour des systèmes abiotiques. On est loin d'une modélisation « pointue » des itinéraires complexes dans lesquels les processus biologiques interviennent dans les réactions chimiques. Il faut continuer à faire des hypothèses ad hoc, à propos de la manière dont les minéraux secondaires se forment dans le sol et l'on ignore nombre d'aspects importants du milieu sol, comportant les variations saisonnières et l'évapo-transpiration.

Dans les modèles prenant en considération l'adsorption, les résultats suggèrent que la théorie de la complexation de surface pourrait avantageusement remplacer les coefficients de répartition, dans la modélisation du transport réactif. En dépit de ce potentiel, il faut noter que la théorie de la complexation

de surface consiste en un traitement purement chimique, tandis que l'approche empirique par K_D intègre à la fois les effets chimiques et les aspects physiques d'un système d'écoulement. Enfin, la simulation par injec-

tion de vapeur ajoute une complication : comment peut-on estimer avec précision les effets des réactions minéralogiques sur la perméabilité ?

I. INTRODUCTION

Many of the most interesting and complex problems in geoscience — from hydrothermal alteration and ore formation to sediment diagenesis and the movement of contaminants in groundwater — involve the reaction of fluids as they flow through the subsurface. To describe such processes quantitatively, geoscientists increasingly turn to numerical models of reactive transport.

Reactive transport modelling is the marriage of mass transport modelling, as applied in hydrology and other fields (e.g. Bird *et al.*, 1960; Javandel *et al.*, 1984), with the geochemical modelling techniques developed since the late 1960s in geoscience (see a review by Bethke, 1996). The coupling of transport and reaction theory, of course, is not new. Palciauskas and Domenico (1976), for example, considered the problem of reactive flows analytically, and modelling of the transport of sorbing solutes using distribution coefficient theory is well established in groundwater hydrology (e.g. Rubin and James, 1973; Valocchi, 1984, 1985; Domenico and Schwartz, 1990). Recently, however, there have been rapid advances (e.g. Lichtner *et al.*, 1996) in developing and applying coupled numerical models that attain the level of chemical sophistication commonly found in geochemical reaction models.

While the natures of mass transport models and geochemical reaction models are well understood within the geoscience community, there has been considerably less discussion about the behaviour of coupled models. In this review, therefore, we first examine some simulations that demonstrate how transport and reaction processes interact in one dimension. Then, in considering the results

of these simulations, we explore the uncertainties and challenges inherent in applying reactive transport models.

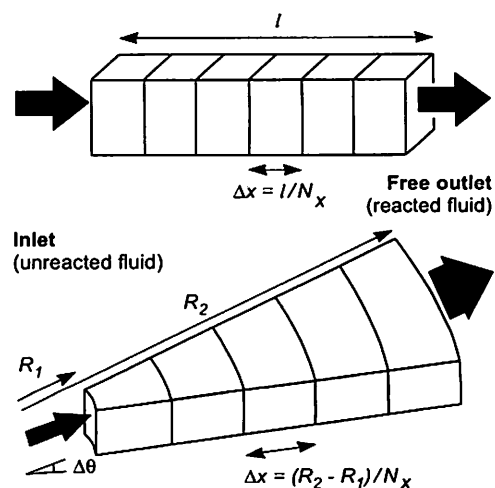
II. MATHEMATICAL MODEL

Numerical models of reactive transport combine the functions of a mass transport model, as commonly applied in hydrogeology, with those of a geochemical reaction model. A reactive transport model can, in fact, be constructed by adding chemical reactions to a transport model or by incorporating transport equations into a reaction model.

Figure 1 shows the conceptual basis for modelling in one dimension. A domain in linear or radial coordinates is discretised into nodal blocks. Unreacted fluid enters one end of the domain, displacing reacted fluid from the other. The calculation follows a time marching procedure. As the initial condition, mass within each nodal block is distributed among the various aqueous species, surface (sorbed) species and minerals. The pro-

Fig. 1 Conceptual basis for one-dimensional reactive transport models in linear (top) and radial (bottom) coordinates. Unreacted fluid enters the domain, displacing reacted fluid toward a free outlet. The length of a linear domain is denoted l ; a radial domain (with angular spacing $\Delta\theta$) extends from radius R_1 to R_2 . To accommodate a numerical solution, the domain is divided into N_x nodal blocks with spacing Δx .

Concept de base pour les modèles de transport réactif à une dimension en coordonnées linéaires (en haut) et radiales (en bas). Un fluide non réactif entre dans le domaine considéré, en déplaçant un fluide réactif vers une sortie libre. La longueur d'un domaine linéaire est représentée par l ; un domaine radial (avec un espacement angulaire $\Delta\theta$) s'observe du rayon R_1 à R_2 . Pour accommoder une solution numérique, le domaine est divisé en N_x blocs nodaux à espacement Δx .



gramme then takes a series of steps forward through time from the initial condition, tracing the chemical evolution of the system as fluid migrates across the domain.

In taking each time step, the programme evaluates four classes of equations:

Transport equations that account for molecular diffusion, hydrodynamic dispersion (i.e. mechanical mixing within the groundwater flow), and advection (transport by the flow itself).

Equilibrium equations that describe the distribution of mass among the aqueous species and minerals that make up the portion of each nodal block to be held in local equilibrium. These relations include mass action and mass balance equations and correlations for estimating activity coefficients.

A *sorption model* that predicts which ions sorb onto mineral surfaces, and in what quantities they do so, if the calculation is to consider surface reactions. Sorption models vary widely; the equations may be simple distribution coefficients or more general models accounting for mass action, mass balance and electrostatic effects for a set of surface complexation reactions.

Kinetic rate laws that predict how rapidly any minerals not held in local equilibrium precipitate or dissolve over the course of the simulation. The rate laws are commonly of a form suggested by transition state theory (e.g. Lasaga, 1984).

The equations in these classes can be evaluated using various solution procedures (Yeh and Tripathi, 1989; Steefel and Lasaga, 1994).

The most straightforward algorithm is to compute how over a time step mass transport affects the composition of each nodal block, and then to evaluate the various chemical equations to determine the distribution of mass at each node. If the kinetic equations are evaluated using fluid compositions averaged between the beginning and end of the time step, the algorithm (used to trace the simulations presented in this paper) is known as "Strang splitting" (Steefel and MacQuarrie, 1996).

Table I lists some of the many reactive transport models in existence. The calcula-

Table I Some codes for modelling reactive transport in porous media.

Software	Reference or contact
HYTEC	van der Lee <i>et al.</i> , 1997
KIRMAT	Gérard <i>et al.</i> , 1996
LEHGC	msiegel@nwer.sandia.gov
MINTRAN	Walter <i>et al.</i> , 1994a, b
MULTIFLO	lichtner@swri.edu
OS3D/GIMRT	Steefel and Yabusaki, 1996
PHREEQC	Parkhurst, 1995

tions in this paper were made with the XIT software package being developed at the University of Illinois, and the LLNL thermodynamic dataset (Delany and Lundeen, 1989). The XIT package is an outgrowth of geochemical modelling techniques described in detail by Bethke (1996).

III. REACTION IN A QUARTZ AQUIFER

In a first calculation (simulation A, **table II**) we consider the effects of rainwater infiltrating at various rates into a quartz (SiO_2) aquifer. Before infiltration, pore fluid in the aquifer is in equilibrium with quartz and hence has a $\text{SiO}_2(\text{aq})$ concentration of about 6 mg/kg. The infiltrating fluid has an initial silica concentration of 1 mg/kg and is therefore undersaturated with respect to quartz.

As the infiltrating fluid invades the aquifer, it reacts to dissolve quartz according to a kinetic rate law

$$r_{\text{qtz}} = A_s k_+ \left(\frac{Q}{K} - 1 \right) \quad (1)$$

of a form suggested by the experiments of Rimstidt and Barnes (1980). Here, r_{qtz} is the reaction rate (mol/s, negative for dissolution), A_s is the surface area of the mineral (cm^2), k_+ is its intrinsic rate constant ($\text{mol}/\text{cm}^2\cdot\text{s}$), and Q and K are the activity product and equilibrium constant for the dissolution reaction

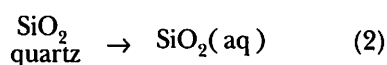


Table II Summary of simulations presented*.

	Domain	Inlet fluid	Initial condition	Transport	Reactions
A	Linear, $l = 100$ m, $N_x = 100$, $T = 25$ °C	1 mg/kg $\text{SiO}_2(\text{aq})$	$\phi = 30$ %, fluid in equil. w/ 70 vol% quartz	$q =$ various values, $\alpha = 10$ cm	Quartz reacts by rate law
B	Linear, $l = 1$ m, $N_x = 100$, $T = 25$ °C	pH 5, 0.5 mg/kg Na^+ , 1.3 mg/kg Cl^- , 0.2 mg/kg K^+ , 1 $\mu\text{g}/\text{kg}$ Al^{+++} , 0.2 mg/kg $\text{SiO}_2(\text{aq})$, $f_{\text{CO}_2} = 10^{-3.5}$	$\phi = 40\%$, $\theta = 25\%$, pH 5, 1 mg/kg Na^+ , 2.5 mg/kg Cl^- , 1 mg/kg K^+ , 1 $\mu\text{g}/\text{kg}$ Al^{+++} , 1 mg/kg $\text{SiO}_2(\text{aq})$, $f_{\text{CO}_2} = 10^{-2}$	$q = 4$ m/year ($v \approx 16$ m/year,) $\alpha = 1$ cm	Quartz, K-feldspar, albite react by rate laws; kaolinite, gibbsite, tridymite can nucleate and form; f_{CO_2} fixed at 10^{-2}
C1	Linear, $l = 100$ m, $N_x = 99$, $T = 25$ °C	pH 6, 0.001 m Na^+ and Cl^- , 100 μm Pb^{++} and Br^- , equil. w/ $\text{Fe}(\text{OH})_3$	$\phi = 30\%$, fluid in equil. w/ 0.015 vol% $\text{Fe}(\text{OH})_3$, pH 6, 0.001 m Na^+ and Cl^- , negligible Pb^{++} and Br^-	$q = 2$ m/year ($v = 6.7$ m/year,) $\alpha = 10$ cm	Sorbate maintains local equilibrium with fluid
C2		Same as C1, except negligible Pb^{++} and Br^- content	Final condition of simulation C1 (100 μm Pb^{++} and Br^-)		
C3		Same as C1, except 100 μm Pb^{++} , Ni^{++} , and Br^-	Same as C1		
D	Radial, $10 \text{ cm} \leq R \leq 2010$ cm, $N_x = 100$	$T = 200$ °C, pH 5, 0.5 mg/kg Na^+ , 2 mg/kg Cl^- , 0.1 mg/kg HCO_3^- , 0.5 mg/kg Ca^{++} , 5 $\mu\text{g}/\text{kg}$ Al^{+++} , 5 mg/kg $\text{SiO}_2(\text{aq})$	$\phi = 35\%$, $T = 40$ °C; fluid in equil. w/ 55 vol% quartz, 5 vol% calcite, and 5 vol% kaolinite; pH 6, 1 m Na^+ , 1 m Cl^- , 0.01 m HCO_3^-	q calculated from evolving k and μ , taking $\Delta\Phi = 2$ MPa; $\alpha = 20$ cm	Quartz reacts by rate law; Ca-smectite can nucleate and form; calcite, kaolinite, and Ca-smectite maintain local equil. with fluid

* f = fugacity, k = permeability, l = length, m = molar concentration, N_x = number of nodal blocks, q = specific discharge, R = radial coordinate, v = groundwater velocity, α = dispersivity, μ = viscosity, Φ = hydraulic potential, ϕ = porosity, θ = water content (vol% fluid in soil).

Table III gives the values taken for the rate constant and surface area.

As the reaction proceeds, the silica concentration and hence the dissolution rate at each point in the aquifer approach a nearly constant (or "plateau") value, as shown in **figure 2**. The plateau represents the balance in the system between the rate at which silica

is transported and how rapidly it reacts. We can quickly calculate (e.g. Lasaga and Rye, 1993; Lichtner, 1996) the time required to approach this state; in this case the relaxation period is about 0.1 year.

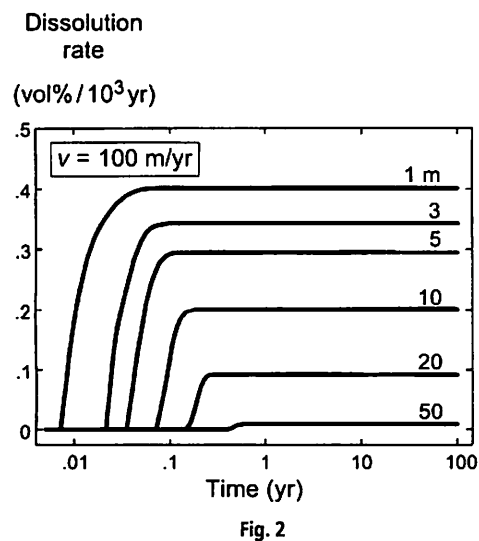
Once the fluid attains its plateau concentration, its composition at any point in the aquifer varies in the simulation only to the

Table III Values assumed for parameters in kinetic rate laws*.

Mineral	k_+ (mol/cm ² s.)	A_{sp} (cm ² /g)	A_{nuc} (cm ² /cm ³)
Quartz*	4.2×10^{-18}	1 000	—
K-feldspar	3×10^{-17}	1 000	—
Albite	1×10^{-16}	1 000	—
Kaolinite	1×10^{-17}	10 000	4 000
Gibbsite	5×10^{-17}	4 000	4 000
Tridymite	6.3×10^{-18}	1 000	4 000

* k_+ = the intrinsic rate constant, A_{sp} = specific surface area, A_{nuc} = area available for nucleation, expressed per cm³ fluid. Data sources: Blum and Stillings (1995), Leamson et al. (1969), Rimstidt and Barnes (1980), Carroll and Walther (1990), Nagy and Lasaga (1992) and White (1995).

* In simulation D, $k_+ = 2.35 \times 10^{-5} \exp(-72\,800/RT_K)$, where R is the gas constant (8.3143 J/K.mol) and T_K is absolute temperature (K).

**Fig. 2**

extent that the quartz surface area [A_s in eq. (1)], and hence the amount of quartz in the aquifer, change. In contrast to the relaxation time already calculated (0.1 year), the time required for the quartz volume to change significantly is more than 10^5 years. Hence, the plateau concentrations remain nearly constant for long periods of time. In reactive transport modelling, nearly steady-state conditions of this type are known (Lichtner, 1988) as “stationary states.”

Figure 3 shows, for differing infiltration rates, how the reaction rate and saturation state for quartz vary across the aquifer once

the system has attained a stationary state. (We obtained these results numerically, but in fact they could have been derived by analytical solution by simplifying the problem only slightly; see Lichtner, 1988.) In all cases, silica dissolves into the fluid as it migrates along the aquifer, causing the quartz saturation state to increase. As a result, the magnitude of the driving force for reaction [$Q/K - 1$ in eq. (1)], and therefore the dissolution rate itself, decreases along the migration path.

This effect is most pronounced for calculations in which the fluid moves slowly. At low flow rates, reaction is concentrated near the inlet, and the fluid approaches local equilibrium with the aquifer after it has migrated only a short distance. The reaction rate rather than the effects of transport controls the fluid chemistry. At rapid flow rates, in contrast, fluid moves through the aquifer too rapidly to accumulate significant quantities of silica or approach equilibrium with quartz, and the reaction rate across the aquifer remains high. Transport effects in such cases dominate the reaction.

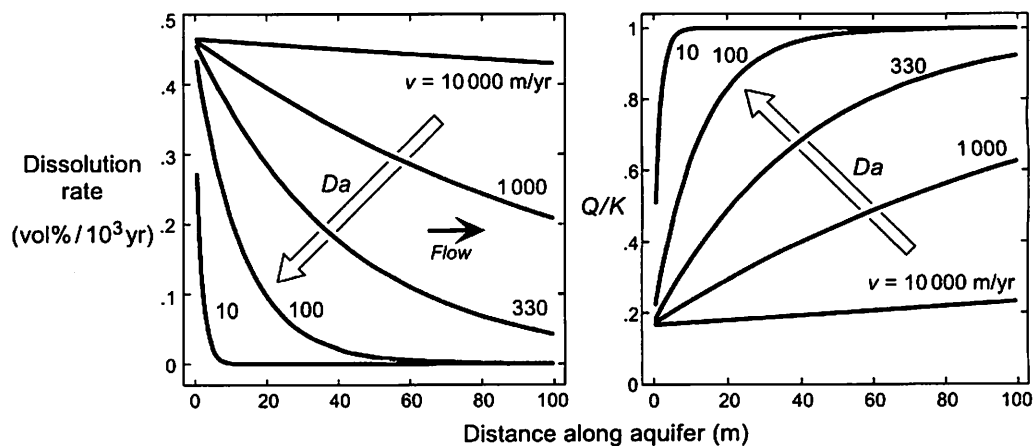
As this example illustrates, the balance between the rates of reaction and transport exerts a primary control on the nature of a reacting flow. This balance is described by the Damköhler number Da (e.g. Knapp, 1989), which represents the rate at which a chemical

Fig. 2 Approach to a stationary state at various positions within an aquifer accepting infiltration of meteoric water, calculated for a groundwater velocity v of 100 m/year (simulation A). The rate at which quartz dissolves (in volume % of the aquifer per 1 000 years) changes from the initial condition of no dissolution to a value that remains nearly constant over long time periods.

Approche vers un état stationnaire à différents points d'un aquifère soumis à l'infiltration d'eau météorique, calculée pour une vitesse de cheminement en profondeur v de 100 m/yr (simulation A). La vitesse à laquelle le quartz se dissout (en % du volume de l'aquifère par 1 000 ans) change depuis une condition initiale de non dissolution jusqu'à une valeur qui demeure à peu près constante sur de longues périodes.

Fig. 3 Variation of the stationary-state reaction rate (left) and saturation state (right) for quartz in an aquifer accepting infiltration of meteoric water, calculated for differing groundwater velocities, v (simulation A). Da is the Damköhler number, which increases in the direction indicated.

Variation de la vitesse de réaction à l'état stationnaire (à gauche) et de l'état saturé (à droite) du quartz dans un aquifère soumis à l'infiltration d'eau météorique, calculée pour différentes vitesses v de cheminement en profondeur (simulation A). Da est le nombre de Damköhler qui croît dans la direction indiquée.



component reacts relative to the rate at which it is transported by advection. For the single-component system considered here, this value is given by

$$Da = \frac{Sk + L}{C_{\text{eq}} v} \quad (3)$$

where S is the mineral surface area per unit fluid volume (cm^{-1}), L is the length of the scale of observation (cm), C_{eq} is the equilibrium concentration (mol/cm^3), and v is the flow velocity (cm/s). Since each of the variables in this equation except v is constant or nearly so in the calculations presented, Da varies inversely with the flow rate. As can be seen in **figure 3**, as Da increases (i.e. as flow diminishes), the reacting system tends toward a state of local equilibrium.

An interesting observation about the results in **figure 3** is that we need to construct a complete reactive transport model under only a relatively narrow range of conditions. At large Da (slow flow), the system approaches local equilibrium and the $\text{SiO}_2(\text{aq})$ activity is given directly by the mass action equation for reaction (2). At small Da (rapid flow), on the other hand, the fluid remains far from equilibrium across the aquifer. In this case, the reaction rate can be computed using a simple "box model." Only when Da falls

between these extremes does a fully coupled model give additional information about the reacting system.

IV. WEATHERING IN A SOIL PROFILE

The weathering of parent rock to produce soil profiles is a process of considerable interest in environmental geoscience because on a global scale weathering reactions constitute an important sink of carbon dioxide (e.g. Berner *et al.*, 1983). The reactions also play significant roles in affecting water quality, groundwater acidification, nutrient cycling, and microbial populations (e.g. White and Brantley, 1995).

In a second numerical experiment (simulation B, **table II**), we use reactive transport theory to predict the distribution of weathering reactions within a soil profile. The soil in our calculation is unsaturated, 1 m thick, and has a porosity of 40% and a moisture content of 25%; it is composed initially of quartz, K-feldspar (KAlSi_3O_8), and albite ($\text{NaAlSi}_3\text{O}_8$). Rainwater in equilibrium with atmospheric CO_2 ($f_{\text{CO}_2} = 10^{-3.5}$, where f is fugacity on an atm scale) recharges the upper surface of the soil and the pore fluid drains from the bottom.

The pore fluid maintains equilibrium with carbon dioxide in the soil gas, the CO_2 fugacity of which is held constant at 10^{-2} to reflect

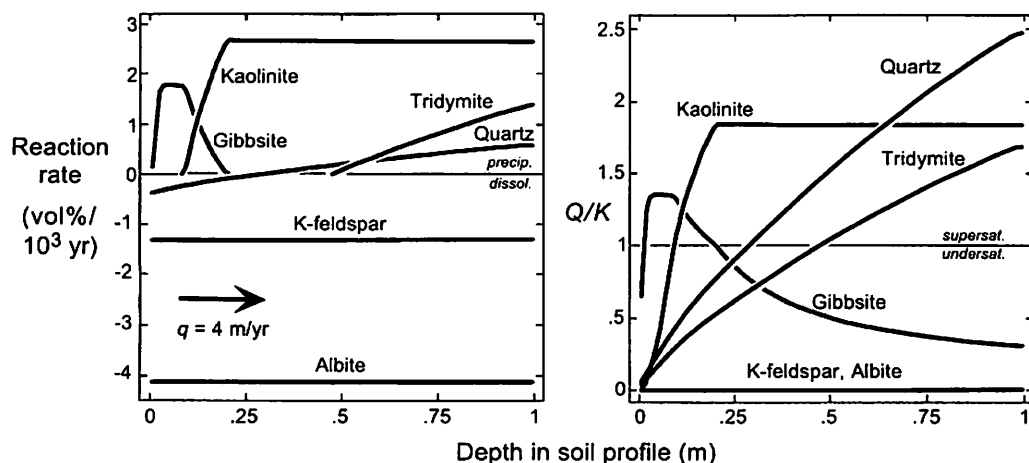
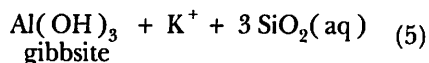
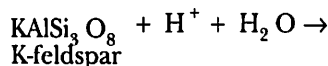
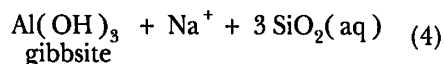
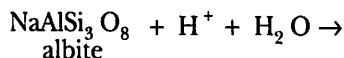


Fig. 4 Stationary-state reaction rates (left) and saturation states (right) for minerals in a soil profile, as predicted by a numerical simulation of weathering (simulation B). Variable q is specific discharge.

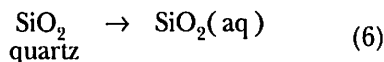
Variation des vitesses de réaction à l'état stationnaire (à gauche) et états saturés (à droite) de minéraux d'un profil de sol, prédits par une simulation numérique de l'altération (simulation B). La variable q est la décharge spécifique.

(in a rough manner) the effects of organic decomposition and root respiration. The minerals kaolinite [$\text{Al}_2\text{Si}_2\text{O}_5(\text{OH})_4$], gibbsite [$\text{Al}(\text{OH})_3$], and tridymite (SiO_2) can form within the soil by heterogeneous nucleation. A kinetic rate law [eq. (1)] sets the rates at which each mineral dissolves or precipitates, according to the parameters listed in table III. In the calculation results (fig. 4), the system quickly approaches a stationary state in which differing reactions occur at various depths.

The simulation shows the separation of silica from aluminium commonly observed within soil profiles. Near the top surface, the feldspar minerals dissolve to produce gibbsite

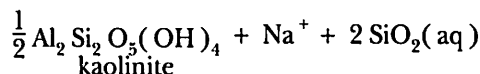
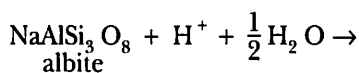


Reflecting their respective rate constants (table III), and in accord with observations in nature, albite dissolves more quickly than K-feldspar. At the same time, quartz dissolves congruently:

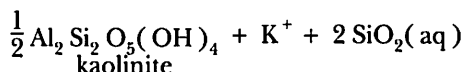
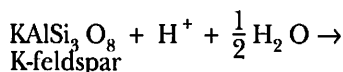


The silica added to solution by reactions (4)–(6) is carried downward by the migrating pore fluid.

As a result, silica activity increases with depth, causing kaolinite to become saturated and precipitate. At about 25 cm, this mineral replaces gibbsite as the sink for the aluminium produced by feldspar dissolution

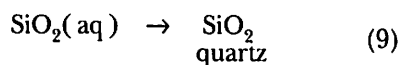


(7)

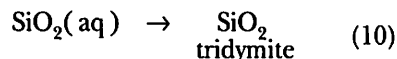


(8)

Quartz becomes saturated at about this depth and begins to precipitate



rather than dissolve. Quartz, however, reacts slowly enough that silica continues to accumulate in solution. About 50 cm into the profile, the silica polymorph tridymite



begins to form, even though it is less stable thermodynamically than quartz. This mineral serves in the calculation as a proxy for opaline silica, a common phase in soils (e.g. Dove, 1995).

The results in figure 4 are of course specific to the drainage rate assumed in the calculation. When flow is varied, the model predicts differing reaction intensities, as discussed in the previous section, and the positions of the various reaction zones shift within the profile.

V. TRANSPORT OF SORBING SPECIES

In many problems, especially those of environmental interest, the sorption of ions onto mineral surfaces controls the transport of minor species. In reactive transport studies, the sorption process is most commonly described in terms of distribution coefficients K_D . Each coefficient K_D gives the ratio of a species' sorbed mass to its concentration in solution. The K_D coefficients are determined empirically for individual cases.

Although the K_D approach is straightforward mathematically and can be integrated readily into models of mass transport, it is somewhat naive from a chemical perspective (e.g. Reardon, 1981). In this section we invoke Dzombak and Morel's (1990) modified double layer model of ion sorption onto hydrous ferric oxide, a strongly sorbing mineral that is widespread in oxidised soils and aquifers. The model differs from the K_D approach in several ways: it is based on reaction theory, predicts the species distribution on the sorbing surface, imposes mass balance over the surface sites, and accounts for electrostatic effects.

The ferric oxide surface, according to Dzombak and Morel's model, contains "strong" and "weak" sites; in their unreacted

forms, they are labelled $>(\text{s})\text{FeOH}$ and $>(\text{w})\text{FeOH}$. There are about 0.005 "strong" and 0.2 "weak" sites per Fe atom. The sites are highly reactive, undergoing protonation, deprotonation, and complexation reactions that yield surface species such as $>(\text{s})\text{FeOH}_2^+$, $>(\text{s})\text{FeO}^-$ and $>(\text{s})\text{FeOPb}^+$.

1. Pb contamination in an oxidised aquifer

In a first calculation (simulation C1, table II), we let water contaminated with inorganic Pb invade an aquifer containing ferric hydroxide $[\text{Fe}(\text{OH})_3]$, a proxy for hydrous ferric oxide. The infiltrating water contains 100 μmolal Pb, which sorbs strongly onto the ferric surface, and an equal amount of Br, which serves in the calculation as a tracer.

In the simulation results (fig. 5), the species migrate through the aquifer in a manner familiar in transport studies. The concentration front for the Br tracer advances with the migrating fluid, becoming less sharp with time under the influence of hydrodynamic (and numerical) dispersion. The Pb front, on the other hand, is retarded relative to the migrating fluid because the lead sorbs strongly onto the ferric surface

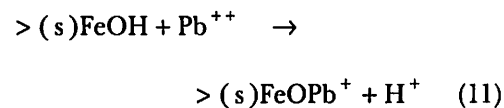
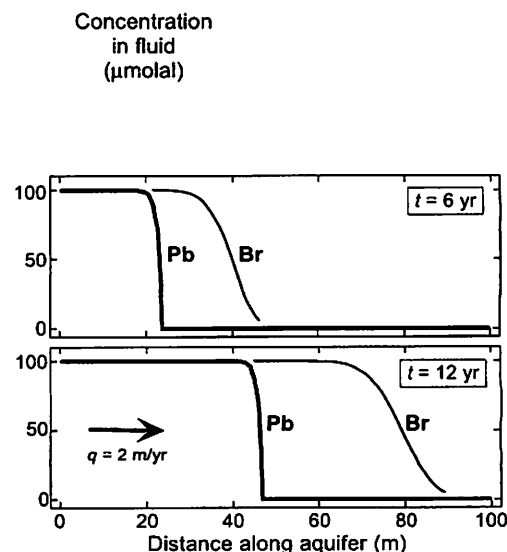


Fig. 5 Aqueous concentrations of Pb and Br as a fluid containing these components in 100 μmolal concentration invades a sorbing aquifer (simulation C1), shown after 6 years (top) and 12 years (bottom) of imbibition. Variable q is specific discharge. The migration front for Pb, which sorbs strongly, is retarded relative to the front for Br, which does not sorb.

Concentrations aqueuses en Pb et Br, quand un fluide contenant ces constituants à la concentration 100 μmolale pénètre dans un aquifère adsorbant (simulation C1), après 6 ans (en haut) et 12 ans (en bas) d'imbibition. La variable q est la décharge spécifique. Le front de migration de Pb qui est fortement adsorbé est en retard par rapport au front de Br qui ne s'adsorbe pas.



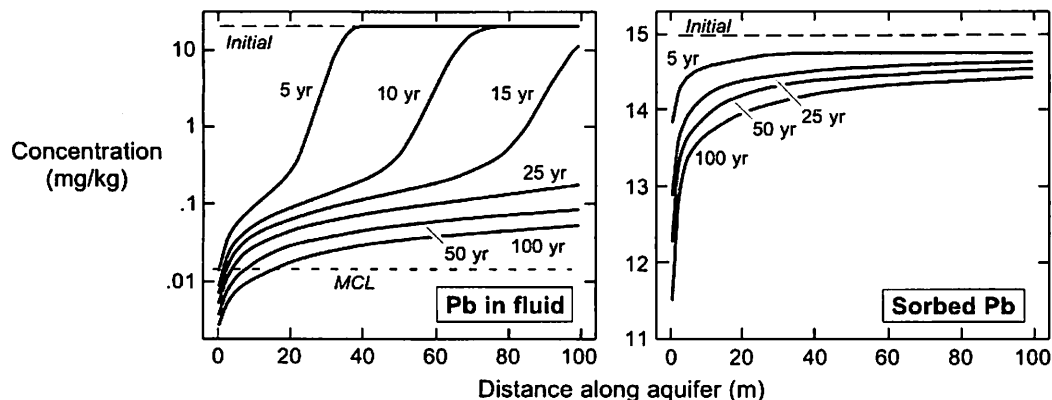


Fig. 6 Concentrations of Pb in the fluid (left) and on the sorbate (right) as clean water flushes a sorbing aquifer contaminated with Pb (simulation C2), at different points in time. Notice that the vertical scales differ between the plots. "MCL" identifies the maximum contamination level, according to US environmental standards.

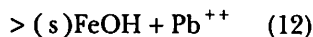
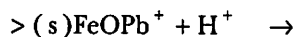
Concentrations en Pb dans le fluide (à gauche) et sur l'adsorbat (à droite), quand de l'eau propre pénètre avec un effet de chasse d'eau dans un aquifère adsorbant contaminé par du Pb (simulation C2), à différents points dans le temps. A noter que les échelles verticales varient selon les données figurées. MCL correspond au niveau de contamination maximum selon les standards d'environnement en usage aux États-Unis.

as the $>(s)\text{FeOPb}^+$ species. The aquifer becomes saturated with Pb after about 25 years. These results differ from those predicted by the K_D approach principally in the steepness of the Pb front.

The reverse process (simulation C2, table II) is more interesting. After the aquifer has been saturated with Pb, a clean fluid passes through it. In the calculation results (fig. 6), the contaminated fluid is flushed from the aquifer and the Pb begins to desorb from the ferric surface. If we had applied the K_D approach, the flushing would accomplish the reverse of the previous calculation (fig. 5): Pb would desorb into the clean water and be carried out of the system, leaving the aquifer nearly pure after about 25 years.

The simulation invoking the double layer model (fig. 6) does not show such behaviour. Instead, Pb desorbs slowly, producing a distinct "tail" of residual contamination in the effluent fluid. After 100 years the aquifer is little remediated, and the Pb content of the fluid remains greater than public health standards allow (the maximum contaminant level, or MCL, in the U.S. is 15 $\mu\text{g}/\text{kg}$).

This "tail" of residual contamination arises when the double layer model is invoked because of the nature of the desorption reaction



As can be seen in figure 7, there are many more complexed [$>(s)\text{FeOPb}^+$] than uncomplexed sites [$>(s)\text{FeOH}$]. By mass ac-

tion, the reaction remains in equilibrium as the Pb^{++} content of the fluid decreases by shifting only slightly to the right. Because the desorption reaction proceeds so slowly, the aquifer will remain contaminated even if it is flushed for thousands of years.

It is interesting to note that "tailing effects" are commonly observed in laboratory and field studies of contaminant transport, and they represent a significant impediment to remediation of polluted groundwater systems (e.g. Brusseau, 1994; National Research Council, 1994). Common explanations for "tailing" call on either non-equilibrium (i.e. rate-limited or kinetic) effects or on physical processes such as the diffusion of the contaminant into the flowing groundwater from areas

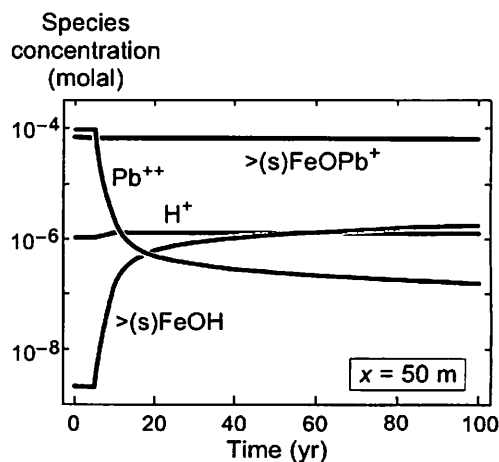
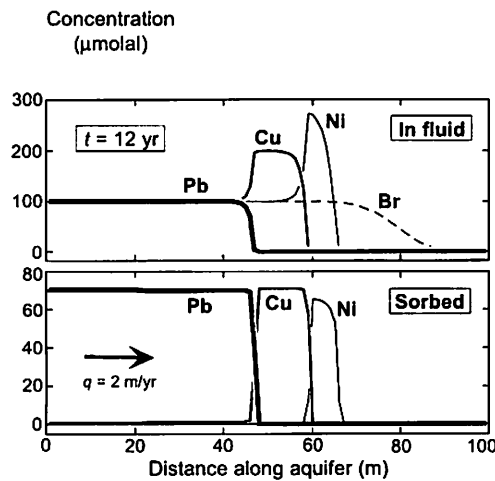


Fig. 7 Concentrations of individual aqueous species (Pb^{++} , H^+) and surface species [$>(s)\text{FeOH}$, $>(s)\text{FeOPb}^+$] over the course of simulation C2, shown at the midpoint of the domain. By the principle of mass action, reaction (12) responds slowly to the introduction of clean water, causing the aquifer to remain contaminated over many hundreds of years.

Concentrations d'espèces aqueuses (Pb^{++} , H^+) et d'espèces de surface [$>(s)\text{FeOH}$, $>(s)\text{FeOPb}^+$] au cours de la simulation C2, observées au centre du domaine étudié. En vertu du principe d'action de masse, la réaction (12) répond lentement à l'introduction d'eau propre, provoquant le maintien de la contamination sur de nombreuses centaines d'années.

Fig. 8 Effect of groundwater containing dissolved Pb, Cu and Ni as it flows through a sorbing aquifer (simulation C3). Br serves in the calculation as a conservative tracer; q is specific discharge. Concentrations of these components in the fluid (top) and on the sorbing surface (bottom) reflect the development and migration of chromatographic zones across the aquifer.

Effet de l'eau souterraine contenant du Pb, du Cu et du Ni dissous, lorsqu'elle parcourt un aquifère adsorbant (simulation C3). Br sert de traceur conservatif dans le calcul ; q est la décharge spécifique. Les concentrations de ces constituants dans le fluide (en haut) et sur la surface adsorbante (en bas) sont le reflet de la progression et de la migration des zones chromatographiques au travers de l'aquifère.



of low permeability, “dead-end” pores, and so on. The calculation presented here, on the other hand, suggests that a chemical process at local equilibrium might contribute to or even account for much of the observed “tailing.”

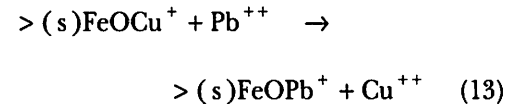
2. Groundwater chromatography

In a final example of the effects of surface complexation, we consider a phenomenon known as “groundwater chromatography” (e.g. Valocchi *et al.*, 1981). Chromatographic effects occur in groundwater flows containing two or more species that sorb with differing strengths; the effects include separation of the ions into individual fronts and development of species concentrations unlike those in the unreacted fluid.

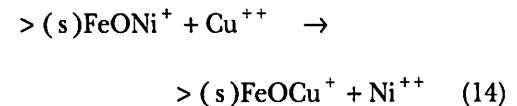
The simulation (C3 in table II) is similar to the model for Pb contamination already presented (simulation C1), except that there are three heavy metal contaminants in the infiltrating solution: Pb, cupric Cu and Ni. Each of these metals is present as a doubly charged cation (Pb^{++} , Cu^{++} and Ni^{++}) and sorbs onto only the “strong” sites on the ferric surface. Hence, the metals compete for sorbing sites. Of the ions, Pb^{++} sorbs most tightly, followed by Cu^{++} , and then Ni^{++} .

In the calculation results (fig. 8), the three metals separate chromatographically. As the fluid passes into the aquifer, Pb sorbs onto the first sites encountered. When the Pb

is depleted, Cu sorbs onto the surface; when Cu is depleted, Ni sorbs. With time, the boundaries between the chromatographic zones migrate along the direction of flow. The fluid continues to supply Pb, which sorbs at the boundary between the Pb and Cu zones. The exchange reaction



displaces Cu from the sorbing surface, adding to the Cu^{++} in solution. Downstream of the boundary, the Cu concentration reflects the sum of the inlet concentrations of Cu and, because of reaction (13), Pb. Similarly, at the boundary between the Cu and Ni zones, the sorption of Cu



supplies Ni to solution. The downstream Ni concentration is the inlet Ni content plus the upstream concentration of Cu. In this way, the Cu and Ni attain concentrations considerably greater than those in the inlet fluid.

Rather than exhibiting simple breakthrough curves, the Cu and Ni concentrations at any point in the simulation may decrease as well as increase with time. In natural systems, which are notably less simple than the calculation presented here, chromatographic effects lead to complex breakthrough curves, the interpretation of which requires an accurate description of the effects of ion sorption.

VI. SIMULATION OF A STEAM FLOOD

In a final calculation (simulation D in table II), we model the effects of a “steam flood” on a clastic petroleum reservoir. Steam flooding is a relatively common procedure designed to lower the viscosity of oil in a reservoir by heating it. The procedure, however, can produce inadvertent results if the injected fluid reacts extensively with the reservoir rock.

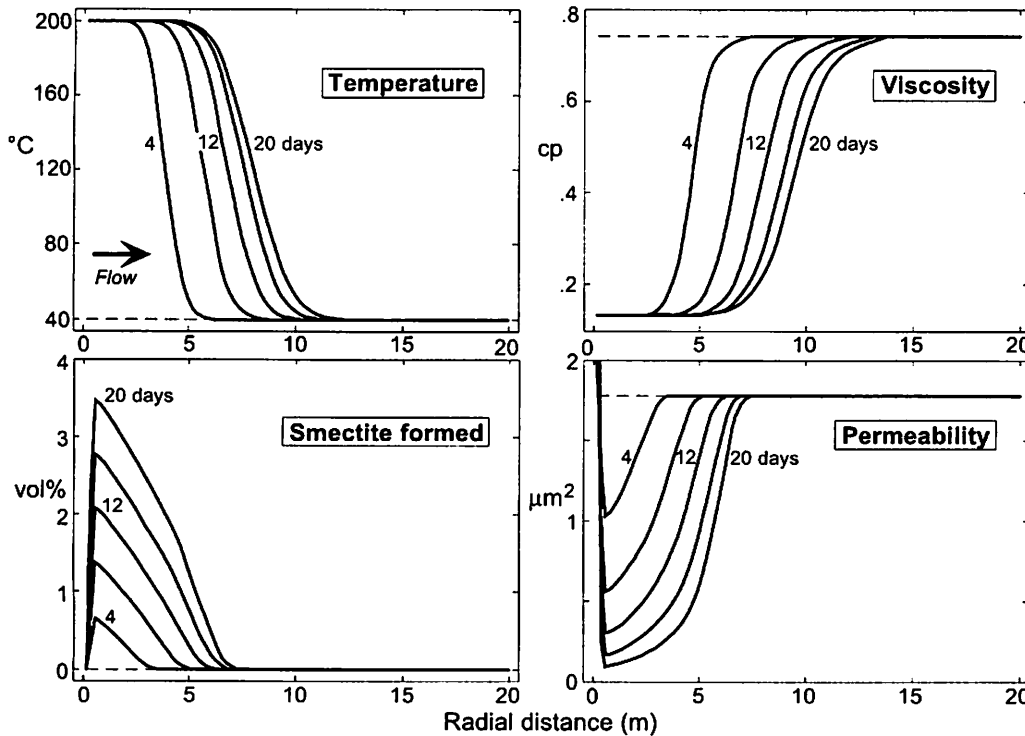
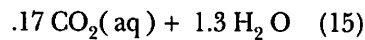
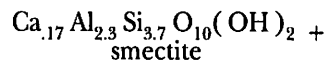
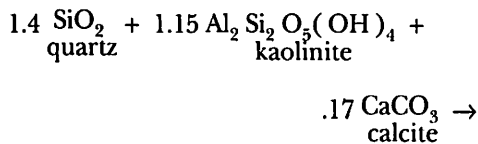


Fig. 9 Effects of a steam flood on a clastic reservoir, according to a numerical model (simulation D). Plots show values of temperature (°C), fluid viscosity ($cp = 10^{-2}$ poise), amount of smectite formed (vol% of medium), and medium permeability (μm^2) across the domain after 4, 8, 12, 16 and 20 days of flooding. Broken lines show initial conditions.

Effets de l'injection de vapeur dans un réservoir clastique selon un modèle numérique (simulation D). Les données figurées correspondent aux valeurs de la température (°C), de la viscosité du fluide ($cp = 10^{-2}$ poise), de la teneur en smectite formée (volume en % du milieu) et de la perméabilité du milieu (μm^2) au travers du domaine étudié, après 4, 8, 12, 16 et 20 jours d'injection. Les lignes en pointillé correspondent aux conditions initiales.

We consider in the simulation a reservoir composed of quartz, calcite and kaolinite. Pressure in the wellbore is 2 MPa higher than ambient, driving 200 °C water radially outward into the formation. The hot water displaces the original fluid and reacts with formation minerals. Quartz reacts according to a kinetic rate law (table III); other minerals maintain local equilibrium with the fluid.

Figure 9 shows how reservoir properties vary over the course of the simulation. The hot water drives a thermal pulse outward into the formation, reaching about 10 m from the wellbore within 20 days. Viscosity decreases in response to the increasing temperature. The reservoir minerals react with the flood to produce smectite in the vicinity of the wellbore according to the reaction



This reaction, in fact, is well known as a laboratory procedure for synthesising smectite (Levinson and Vian, 1966).

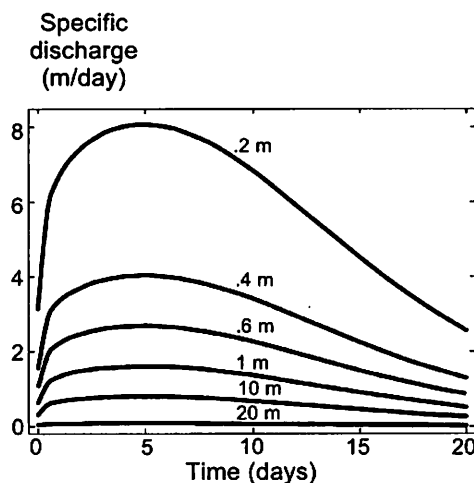
Since smectite is a hydrated or "swelling" clay, its presence in a formation generally has a strong negative effect on permeability. In the simulation, the correlation

$$\log k = 15\phi - 40X_{sm} - 5 \quad (16)$$

accounts for this effect. Here, k is permeability in μm^2 , ϕ is porosity (expressed as a fraction), and X_{sm} is the volume fraction of smectite in the formation. Since in this equation permeability correlates negatively with the smectite content of the formation, its value decreases with time in the simulation, especially near the wellbore where in a radial flow system free flow is most critical.

Fig. 10 Variation of fluid discharge with time over the course of simulation D, at various radial distances. Discharge decreases with distance from the wellbore in the radial flow regime. Flow rate in the simulation initially increases due to a decrease in fluid viscosity, then decreases in response to diminishing permeability near the wellbore.

Variation de la décharge du fluide en fonction du temps au cours de la simulation D à différentes distances radiales. La décharge diminue en fonction de la distance au puits de forage, en régime d'écoulement radial. La vitesse d'écoulement, dans la simulation, commence d'abord à augmenter en raison d'une diminution de viscosité du fluide, puis décroît en réponse à une diminution de la perméabilité près du puits.



Discharge through the formation varies with time as the viscosity and permeability change (fig. 10). Initially, the discharge increases in response to the falling viscosity near the wellbore. With time, however, this effect is counterbalanced by the loss of permeability owing to smectite growth. After 20 days, fluid migrates through the formation more slowly than at the onset of steam flooding. The net effect on petroleum production would depend on the extent to which the treatment benefits oil mobility, but the mineralogic damage to the formation in this case is likely to exert a significant control on the production rate.

VII. DISCUSSION

Reactive transport modelling is a powerful tool for analysing a broad variety of important problems in geoscience. The simulations presented in this paper provide a glimpse of how such modelling might be applied and the nature of the modelling results that can be expected. As in any useful modelling study, however, the simulations also serve to point out deficiencies in the model formulation as well as gaps in the underlying theory and the data needed to implement that theory. Indeed, the modelling incorporates many of the most stubborn areas of uncertainty in groundwater hydrology and geochemistry.

In the model of rainwater invading a quartz aquifer (simulation A), for example, the fluid approaches chemical equilibrium with the aquifer within a short interval of time, even though shallow groundwater in nature seldom equilibrates with this mineral. This discrepancy might be explained by occlusion of the surface area of the mineral by other minerals, organic matter, biofilms, and so on. More significantly, the silica content of groundwater may be strongly affected by reactions with other silica-bearing minerals. Clays and zeolites, for example, may react so much more quickly than quartz that they control the silica composition of the fluid even when present in only minor quantities. Constructing an accurate model in this case may require us to obtain kinetic rate laws for a number of minerals, not just for the predominant mineral in the aquifer.

It is worth noting as well that flow in natural aquifers is uneven, with groundwater migrating quickly through some parts of a formation and slowly through others. As a result of such "bypassing," we should not expect to find a single Damköhler number for flow through natural formations. Instead, the relative rates of reaction and transport should vary within any portion of the aquifer, and so, therefore, should fluid composition. The problem of accounting for bypassing in reactive flows has not been adequately addressed to date.

Further complications arise in interpreting the results of the weathering model (simulation B). A soil is the site of intense biological activity, but nearly all kinetic data are reported for abiotic systems. To attempt to account for effects such as microbial activity, root respiration and organic decay, we set an elevated CO_2 fugacity, but this assumption is ad hoc and cannot be expected to truly reflect the complex ways in which biological processes mediate chemical reactions. We make further ad hoc assumptions about how secondary minerals nucleate in the soil, since kinetic theory to date provides little guidance about modelling heterogeneous nucleation in natural systems. We might note also that

the model ignores many significant aspects of the soil environment, including seasonal variations and evapotranspiration.

The results of models considering ion sorption (simulations C1–C3) suggest that surface complexation modelling might profitably replace distribution coefficient theory (the K_D approach and its variants) in reactive transport modelling, as in Kohler *et al.* (1996). An advantage of surface complexation theory is that it may be applicable over a range of chemical conditions, such as across changes in pH and salinity. In addition, the theory can explain “non-ideal” behaviour such as tailing, as shown in figure 6.

Despite this potential, it should be noted that surface complexation theory is a purely chemical treatment, with its parameters commonly (although not necessarily) derived in

the laboratory. Coefficients for the various implementations of the K_D approach, on the other hand, are fit to best represent observations for a specific problem at a given scale of observation. The K_D approach, therefore, integrates both chemical effects and physical aspects of the problem. For this reason, application of surface complexation theory to explain specific datasets may require better understanding of physical phenomena including bypassing, dispersion and diffusion through dead-end pores and organic matter.

Finally, the steam flood model (simulation D) raises an additional complication: how can we estimate the effects of chemical reactions on the permeability of the medium? The calculations presented rely on an empirical relation [eq. (16)], but such correlations are of unknown generality and not always available.

Acknowledgements: This research was initiated in 1995 when the author was on sabbatical leave at the Ecole des Mines de Paris in Fontainebleau under the sponsorship of the Académie des Sciences, Elf Aquitaine and the University of Illinois. The author appreciates the hospitality extended by the Centre d'Informatique Géologique during this period. Software development for this project was supported by a consortium of industry and governmental laboratories, including Amoco Production Research Company, ARCO Oil and Gas Company, Chevron Oil Field Research, Conoco, Inc., Exxon Production Research Company, Hewlett-Packard, Japan National Oil Corporation, Lawrence Livermore National Laboratory, Marathon Oil Company, Mobil Research and Development, Sandia National Laboratory, SiliconGraphics Computer Systems, Texaco USA and the US Geological Survey.

- BERNER, R.A., LASAGA, A.C. and GARRELS, R.M., 1983. The carbonate-silicate geochemical cycle and its effect on atmospheric carbon dioxide over the past 100 million years, *Am. J. Sci.*, 283, pp. 641–683.
- BETHKE, C.M., 1996. *Geochemical reaction modeling, concepts and applications*, Oxford University Press, New York, 397 pp.
- BIRD, R.B., STEWART, W.E. and LIGHTFOOT, E.N., 1960. *Transport phenomena*, Wiley, New York, 680 pp.
- BLUM, A.E. and STILLINGS, L.L., 1995. Feldspar dissolution kinetics, *Rev. Mineral.*, 31, pp. 291–351.
- BRUSSEAU, M.L., 1994. Transport of reactive contaminants in heterogeneous porous media, *Rev. Geophys.*, 32, pp. 285–313.
- CARROLL, S.A. and WALTHER, J.V., 1990. Kaolinite dissolution at 25 °C, 60 °C, and 80 °C, *Am. J. Sci.*, 290, pp. 797–810.
- DELANY, J.M. and LUNDEEN, S.R., 1989. The LLNL thermochemical database, Lawrence Livermore National Laboratory Report UCRL-21658, 150 pp.
- DOMENICO, P.A. and SCHWARTZ, F.W., 1990. *Physical and chemical hydrogeology*, Wiley, New York, 824 pp.
- DOVE, P.M., 1995. Kinetic and thermodynamic controls on silica reactivity in weathering environments, *Rev. Mineral.*, 31, pp. 235–290.
- DZOMBAK, D.A. and MOREL, F.M.M., 1990. *Surface complexation modeling, hydrous ferric oxide*, Wiley, New York, 393 pp.
- GÉRARD, F., CLÉMENT, A., FRITZ, B. and CROVISIER, J.-L., 1996. Introduction des phénomènes de transport dans le modèle thermo-cinétique KINDIS: le modèle KIRMAT, *C.R. Acad. Sci. Paris*, 322, Séries IIa, pp. 377–384.
- JAVANDEL, I., DOUGHTY, C. and TSANG, C.F., 1984. *Groundwater transport*, American Geophysical Union, Washington DC, 228 pp.
- KNAPP, R.B., 1989. Spatial and temporal scales of local equilibrium in dynamic fluid-rock systems, *Geochim. Cosmochim. Acta*, 53, pp. 1955–1964.
- KOHLER, M., CURTIS, G.P., KENT, D.B. and DAVIS, J.A., 1996. Experimental investigation and modeling of uranium (VI) transport under variable chemical conditions, *Water Resour. Res.*, 32, pp. 3539–3551.
- LASAGA, A.C., 1984. Chemical kinetics of water-rock interactions, *J. Geophys. Res.*, 89, pp. 4009–4025.
- LASAGA, A.C. and RYE, D.M., 1993. Fluid flow and chemical reaction kinetics in metamorphic systems, *Am. J. Sci.*, 293, pp. 361–404.
- LEAMNISON, R.N., THOMAS, J., Jr. and EHRLINGER, H.P., III, 1969. A study of the surface areas of particulate microcrystalline silica and silica sand, *Illinois State Geol. Surv. Circ.*, 444, 12 pp.
- LEVINSON, A.A. and VIAN, R.W., 1966. The hydrothermal synthesis of montmorillonite group minerals from kaolinite, quartz and various carbonates, *Am. Mineral.*, 51, pp. 495–498.

REFERENCES

- LICHTNER, P.C., 1988. The quasi-stationary state approximation to coupled mass transport and fluid-rock interaction in a porous medium, *Geochim. Cosmochim. Acta*, 52, pp. 143–165.
- LICHTNER, P.C., 1996. Continuum formulation of multicomponent-multiphase reactive transport, *Rev. Mineral.*, 34, pp. 1–81.
- LICHTNER, P.C., STEEFEL, C.I. and OELKERS, E.H. (eds), 1996. Reactive transport in porous media, *Rev. Mineral.*, 34, 438 pp.
- NAGY, K.L. and LASAGA, A.C., 1992. Dissolution and precipitation kinetics of gibbsite at 80 °C and pH 3, the dependence on solution saturation state, *Geochim. Cosmochim. Acta*, 56, pp. 3093–3111.
- NATIONAL RESEARCH COUNCIL, 1994. *Alternatives for ground water cleanup*, National Academy Press, Washington, 315 pp.
- PALCIAUSKAS, V.V. and DOMENICO, P.A., 1976. Solution chemistry, mass transfer, and the approach to chemical equilibrium in porous carbonate rocks and sediments, *Geol. Soc. Am. Bull.*, 87, pp. 207–214.
- PARKHURST, D.L., 1995. User's guide to PHREEQC, a computer model for speciation, reaction-path, advective-transport and inverse geochemical calculations, *U.S. Geol. Surv., Water-Resources Investigations Report*, 95–4227, 143 pp.
- REARDON, E.J. 1981. K_{fs} – Can they be used to describe reversible ion sorption reactions in contaminant migration? *Ground Water*, 19, pp. 279–286.
- RIMSTIDT, J.D. and BARNES, H.L., 1980. The kinetics of silica-water reactions, *Geochim. Cosmochim. Acta*, 44, pp. 1683–1700.
- RUBIN, J. and JAMES, R.V., 1973. Dispersion-affected transport of reacting solutes in saturated porous media: Galerkin method applied to equilibrium controlled exchange in unidirectional steady groundwater flow, *Water Resour. Res.*, 9, pp. 1332–1356.
- STEEFEL, C.I. and LASAGA, A.C., 1994. A coupled model for transport of multiple chemical species and kinetic precipitation/dissolution reactions with application to reactive flow in single phase hydrothermal systems, *Am. J. Sci.*, 294, pp. 529–592.
- STEEFEL, C.I. and MacQUARRIE, K.T.B., 1996. Approaches to modeling of reactive transport in porous media, *Rev. Mineral.*, 34, pp. 83–129.
- STEEFEL, C.I. and YABUSAKI, S.B., 1996. OS3D/GIMRT, software for modeling multicomponent-multidimensional reactive transport, Pacific Northwest National Laboratory Report, 58 pp.
- VALOCCHI, A.J., 1984. Describing the transport of ion-exchanging contaminants using an effective K_d approach, *Water Resour. Res.*, 20, pp. 499–503.
- VALOCCHI, A.J., 1985. Validity of the local equilibrium assumption for modeling sorbing solute transport through homogeneous soils, *Water Resour. Res.*, 21, pp. 808–820.
- VALOCCHI, A.J., STREET, R.L. and ROBERTS, P.V., 1981. Transport of ion-exchanging solutes in groundwater, chromatographic theory and field simulation, *Water Resour. Res.*, 17, pp. 1517–1527.
- VAN DER LEE, J., LEDOUX, E., DE MARSILY, G., VINSOT, A., VAN DE WEERD, H., LEIJNSE, A., HARMAND, B., RODIER, E., SARDIN, M., DODDS J. and HERNANDEZ BENMTEZ, A., 1997. Development of a model for radionuclide transport by colloids in the geosphere, Commission of the European Communities (CEC), in: *Nuclear Science and Technology*, in press.
- WALTER, A.L., FRIND, E.O., BLOWES, D.W., PTACEK, C.J. and MOLSON, J.W., 1994a. Modeling of multicomponent reactive transport in groundwater, 1., Model development and evaluation, *Water Resour. Res.*, 30, pp. 3137–3148.
- WALTER, A.L., FRIND, E.O., BLOWES, D.W., PTACEK, C.J. and MOLSON, J.W., 1994b. Modeling of multicomponent reactive transport in groundwater, 2., Metal mobility in aquifers impacted by acidic mine tailings discharge, *Water Resour. Res.*, 30, pp. 3149–3158.
- WHITE, A.F., 1995. Chemical weathering rates of silicate minerals in soils, *Rev. Mineral.*, 31, pp. 406–461.
- WHITE, A.F. and BRANTLEY, S.L., 1995. Chemical weathering rates of silicate minerals, *Rev. Mineral.*, 31, 583 pp.
- YEH, G.T. and TRIPATHI, V.S., 1989. A critical evaluation of recent developments in hydrogeochemical transport models of reactive multichemical components, *Water Resour. Res.*, 25, pp. 93–108.